Int. J. Dev. Biol. 65: 523-536 (2021)
https://doi.org/10.1387/ijdb.210087yl

THE INTERNATIONAL JOURNAL OF DEVELOPMENTAL BIOLOGY
www.intjdevbiol.com

A screen of kinase inhibitors reveals a potential role of Chk1 in regulating *Hydra* head regeneration and maintenance

YUNJIN LEE, VARUN MUDDALURU, SHIRAZ ANWAR, JOANNA YVONNE WILSON and ANA REGINA CAMPOS*

McMaster University, Department of Biology, School of Interdisciplinary Sciences, Ontario, Canada

ABSTRACT The cnidarian *Hydra* possesses remarkable regenerative capabilities which allow it to regrow lost or damaged body parts in a matter of days. Given that many key regulators of regeneration and development are evolutionarily conserved, *Hydra* is a valuable model system for studying the fundamental molecular mechanisms underlying these processes. In the past, kinase inhibitors have been useful tools for determining the role of conserved signaling pathways in *Hydra* regeneration and patterning. Here, we present a systematic screen of a commercially available panel of kinase inhibitors for their effects on *Hydra* regeneration. Isolated *Hydra* gastric segments were exposed to 5 μM of each kinase inhibitor and regeneration of the head and foot regions were scored over a period of 96 hours. Of the 80 kinase inhibitors tested, 28 compounds resulted in abnormal regeneration. We directed our focus to the checkpoint kinase 1 (Chk1) inhibitor, SB 218078, considering the role of Chk1 in G2 checkpoint regulation and the importance of G2-paused cells in *Hydra* regeneration. We found that *Hydra* exposed to SB 218078 were unable to regenerate the head and maintain head-specific structures. Furthermore, SB 218078-treated *Hydra* displayed a reduction in the relative proportion of epithelial cells; however, no differences were seen for interstitial stem cells or their derivatives. Lastly, exposure to SB 218078 appeared to have no impact on the level of mitosis or apoptosis. Overall, our study demonstrates the feasibility of kinase inhibitor screens for studying *Hydra* regeneration processes and highlights the possible role for *Hydra* Chk1 in head regeneration and maintenance.

KEY WORDS: *Hydra, regeneration, kinase inhibitors, small molecule screen, Chk1*

Introduction

Regeneration is a complex biological process by which cells, tissues or body parts lost to injury and/or daily wear and tear activities are restored. It is deemed to be a key ancestral trait that is broadly yet inconsistently exhibited throughout the animal kingdom. Many invertebrates and primitive vertebrate species possess proficient regenerative capabilities that allow them to restore missing body structures (Mehta and Singh, 2019). Among the regeneration competent species, the freshwater cnidarian *Hydra* has captured the attention of developmental biologists for more than 200 years (Galliot, 2012). This primitive metazoan can regenerate a complete adult organism from a minor segment of the original body. Moreover, *Hydra* that is experimentally dissociated into single cells can reaggregate into clumps forming an intact animal within a few days (Vogg *et al.*, 2019).

Hydra possesses a radially symmetric, tubular body consisting of a head, body column, and basal disc. The head is made up of the hypostome (mouth region) and a ring of tentacles that capture prey, while the basal disc (foot) secretes a mucous that allows the animal to attach to various surfaces. The overall *Hydra* body is essentially composed of two epithelial cell layers, the ectoderm (epidermis) and endoderm (gastrodermis) which are separated by acellular mesoglea layer. Three stem cell lineages are present in *Hydra*: unipotent ectodermal and endodermal epithelial cells, and multipotent interstitial stem cells (Hobmayer *et al.*, 2012). The outer body layer is composed of ectodermal epithelial stem cells, while the inner gastric lining constitutes of endodermal epithelial stem cells. Interstitial stem cells are distributed between the two layers and concentrated in the body column. These multipotent stem cells give rise to nematocytes, neurons, gland cells and gametes (Hobmayer *et al.*, 2012). More recently, whole-body single-cell transcriptomics of *Hydra* revealed that interstitial stem cells give

Abbreviations used in this paper: Chk1, Checkpoint Kinase 1; DDR, DNA Damage Response; DEI, Drug Exposure Impact; Hpe, Hours post exposure.

***Address correspondence to:** Ana Regina Campos. McMaster University, Hamilton, L8S 4K1, Ontario, Canada.
Tel: (905) 525-9140 ext. 21509. E-mail: camposa@mcmaster.ca - https://orcid.org/0000-0002-6001-7942

Submitted: 10 June, 2021; *Accepted:* 10 August, 2021; *Published online:* 10 August, 2021.

ISSN: Online 1696-3547, Print 0214-6282

rise to a bipotential neuron/gland progenitor in the ectoderm that traverses the mesoglea to provide the endoderm with neurons and gland cells (Siebert *et al.*, 2019).

Hydra is capable of both asexual and sexual reproduction. During optimal environmental conditions, *Hydra* undergoes asexual reproduction through the process of budding. In contrast, when exposed to various environmental stressors, it engages in gametogenesis and sexual reproduction (Buzgariu *et al.*, 2015). Furthermore, *Hydra* can maintain constant body size throughout its lifetime due to the synchronous gain and loss of cells. Epithelial stem cells have an average cycling time of 3-4 days, while interstitial cells have a cell cycle duration of 24-30 hours (Hobmayer *et al.*, 2012; Buzgariu *et al.*, 2014). While tissue growth is constant in the *Hydra* body column, there is a simultaneous loss of cells through sloughing at the buds, tentacles, and basal ends (Bode, 1996). Given this spatial restriction of stem cell cycling, *Hydra* is said to be "immortal" in the central body column, yet simultaneously aging at the extremities (Schenkelaars *et al.*, 2018).

Any isolated segment of the *Hydra* body column is capable of regenerating into an intact, viable animal maintaining the original oral aboral polarity. The central body column of *Hydra* is composed of large stocks of adult stem cells paused in G2 stage of the cell cycle, forming a constitutive pro-blastema, ready to divide upon injury (Galliot *et al.*, 2018). In contrast, the apical and basal extremities of *Hydra* are enriched in terminally differentiated cells and thus incapable of regenerating missing structures. Upon mid-gastric bisection, head regeneration is achieved by a wave of injury-induced cell death and compensatory proliferation (Galliot *et al.*, 2018). In contrast, following decapitation, apical head regeneration can proceed in the absence of cell proliferation and relies on a morphallactic mode of regeneration (Galliot and Chera, 2010). Additionally, *Hydra* regeneration can be accomplished with epithelial stem cells only, as the ablation of the interstitial stem cell lineage does not prevent regeneration following bisection (Marcum and Campbell, 1978; Sugiyama and Fujisawa, 1978). The regeneration capacity of such epithelial *Hydra* may be attributed to the ability of epitheliomuscular cells to modify their transcriptomic programme upon elimination of the cycling interstitial cells (Wenger *et al.*, 2016).

Remarkably, *Hydra* share more genes with humans than the popular model organisms, *Drosophila melanogaster* and *Caenorhabditis elegans* (Wenger and Galliot, 2013a). Sequencing and in-depth analysis of the *Hydra* genome has estimated that it encodes approximately 20,000 protein coding genes, which is similar to the number found in the human genome (Chapman *et al.*, 2010). Moreover, all major bilaterian signalling pathways including Wnt, transforming growth factor-β, Hedgehog, receptor tyrosine kinase and Notch have been identified in *Hydra* (Chapman *et al.*, 2010). To interrogate the function of genes underlying *Hydra* regeneration, several molecular tools have been developed including double-stranded RNA-mediated interference (dsRNAi) and stable transgenesis (Mehta and Singh, 2019). Nonetheless, limitations include the high mortality associated with dsRNAi approaches and the variability in success rate of transgenesis (Technau and Steele, 2011; Klimovich *et al.*, 2019). Furthermore, a major caveat in performing functional genomics in cnidarian models is the difficulty in generating heritable genetic mutations that result in true knockouts/knockins. However, this may rapidly change as the application of CRISPR-Cas9 system for genome-editing in *Hydra* has shown great promise (Lommel *et al.*, 2017).

A long-standing approach to identify key signaling molecules of *Hydra* regeneration is the use of pharmacological modulators. In particular, kinase inhibitors identified on the basis of their ability to disrupt regeneration have provided valuable insight into the normal role of the target signaling pathway in *Hydra* patterning and regeneration. For instance, the induction of Wnt/β -catenin signaling by treatment with alsterpaullone, a specific glycogen synthase kinase-3β (GSK-3β) inhibitor, induces the expression of head organizer genes and formation of ectopic tentacles along the *Hydra* body column (Broun *et al.*, 2005). Likewise, pharmacological inhibitors of protein kinase C (PKC), mitogen-activated protein kinase (MEK), Src tyrosine kinase, extracellular signal-regulated kinase (ERK), phosphoinositide 3-kinase (PI3K), vascular endothelial growth factor (VEGF), and fibroblast growth factor (FGF) were used to implicate the importance of these signaling pathways in *Hydra* head regeneration (Cardenas *et al.*, 2000; Cardenas and Salgado, 2003; Manuel *et al.*, 2006; Arvizu *et al.*, 2006; Turwankar and Ghaskadbi, 2019). Using similar paradigms, Glauber and colleagues demonstrated the feasibility of small molecule screens for dissecting *Hydra* patterning processes. Through this approach, they identified a novel molecule, DAC-2-25, which caused homeostatic

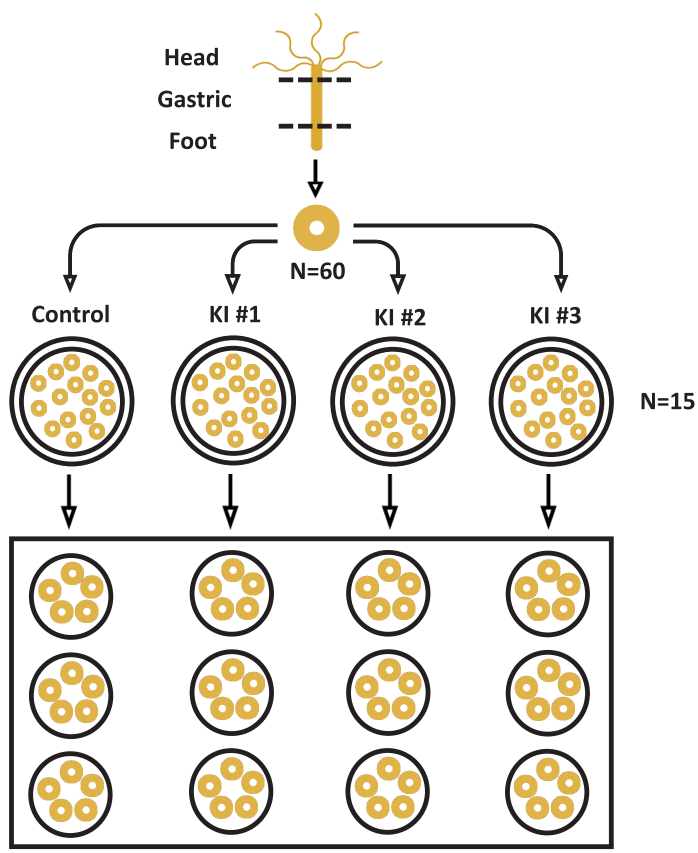

Fig. 1. Schematic illustration of the 80 kinase inhibitor screen. *Three kinase inhibitors (KIs) were tested per 12-well plate. For each plate, 60* Hydra *gastric regions were isolated by removing the head and foot. For each treatment, 15 gastric regions were rinsed with the respective solution (KI #1, KI #2, KI #3, or control) before dividing them into 3 wells (5 gastric regions per well) containing the respective exposure solutions. Control replicates were exposed to 1% DMSO alone and included on every plate.*

transformation of the *Hydra* body column into a tentacle zone (Glauber *et al*., 2013). Therefore, to identify novel regulators and signal transduction pathways underlying the *Hydra* regeneration processes, we screened a commercially available panel of 80 kinase inhibitors (Tocriscreen Kinase Inhibitor Toolbox Cat. No. 3514) for their impact on *Hydra* regeneration. Our screen identified 28 compounds that cause abnormal regeneration from which the Chk1 inhibitor, SB 218078, was prioritized for additional follow-up analysis. We show that SB 218078-treated *Hydra* were incapable of head-specific regeneration and maintenance, which may be in part due to a reduction in the relative proportion of epithelial stem cells.

Results

The use of kinase inhibitors to identify potential novel regulators of Hydra *regeneration*

To identify novel signaling pathways underlying *Hydra* regeneration, an unbiased screen of 80 kinase inhibitors (Tocriscreen Kinase Inhibitor Toolbox Cat. No. 3514) was performed. Isolated gastric segments were exposed to 5 μM of each kinase inhibitor, following the screen set up as illustrated (Fig. 1). After 96-hours, regeneration of each *Hydra* gastric segment was scored on a scale of 0 – 10 using the Wilby 1988 classification scheme (Quinn *et al*., 2012). Given that kinase inhibitors were supplied as pre-dissolved DMSO solutions, control *Hydra* were exposed to equivalent solvent concentrations to those in the inhibitor groups. The difference between the average regeneration score of each exposure group and its respective control was calculated to generate the Drug Exposure Impact (DEI) for each kinase inhibitor; an increasingly negative DEI value suggests a progressively negative impact of the kinase inhibitor on regeneration. Additionally, *Hydra* morphology following 96-hour exposure to each kinase inhibitor was noted. In total, four distinct morphological categories were observed: (1) complete regeneration (Fig. 2A), (2) partial regeneration - presence of shortened tentacles and body column (Fig. 2B), (3) arrested regeneration - no formation of a head and foot (Fig. 2C), and (4) disintegration - the breakdown of *Hydra* tissues into debris (Fig. 2D). Of the 80 kinase inhibitors, 24 inhibitors were associated with complete regeneration, 23 inhibitors with partial regeneration, 5 inhibitors with arrested regeneration, and 28 inhibitors with disintegration. DEI values for complete regeneration ranged between -1.07 and 1.2; partial regeneration ranged between -4.4 and 0.6; arrested regeneration ranged between -7.67 and -4; and disintegration ranged between -10 and -7.8 (Fig. 3).

Next, the 80 kinase inhibitors were organized by the main signal transduction pathway that they are presumed to target (Table. S1). Of the various pathways, kinase inhibitors of the DNA Damage Response (DDR) were of particular interest for the following reasons: (1) exposure to all of the DDR inhibitors prevented normal regeneration, (2) many components of the DNA repair mechanism are evolutionarily conserved in *Hydra* (Wenger and Galliot, 2013b; Barve *et al*., 2013a; Barve *et al*., 2013b; Pekhale *et al*., 2017; Galande *et al*., 2018; Galande *et al*., 2021), and (3) the robust self-renewing potential of *Hydra* have been attributed to the efficiency of its DNA repair mechanisms (Dańko *et al.,* 2015; Haval *et al*., 2020). We decided to further pursue SB 218078, a potent adenosine triphosphate (ATP)-competitive inhibitor of the G2 checkpoint protein kinase, Chk1 (IC_{50} of 15 nM for human Chk1) (Jackson *et al*., 2000; Kawabe, 2004; Chen *et al*., 2006). SB 218078 is also a less potent inhibitor of cyclin-dependent protein kinase Cdc2 and PKC (IC_{50} values of 250 nM and 1000 nM for human Cdc2 and PKC, respectively), which are also involved in G2 checkpoint regulation (Jackson *et al*., 2000; Barboule *et al*., 1999).

Activation of Chk1 is known to lead to G2 cell cycle arrest and the accumulation of G2 cells has been positively linked to regeneration in many species (Buzgariu *et al.,* 2018; Bedelbaeva *et al.,* 2010; Rao *et al.,* 2009). To explore the likelihood that Chk1 is the target of SB 218078 in *Hydra*, we compared *Hydra vulgaris* Chk1 (XM_012700247.1) to human Chk1 (Isoform1; NP_001107593.1). These proteins are 51% identical and 66% similar based on EMBOSS Needle Pairwise Sequence Alignment (Madeira *et al*., 2019). Additionally, important amino acid residues are conserved between *Hydra* and human Chk1, including the ATP-binding pocket residue, Glu85, which participates in a protein-ligand hydrogen bond in the co-crystal structure of SB 218078 and human Chk1 (Zhao *et al*., 2002), and the 'gatekeeper' residue, Leu84, which controls selectivity for small molecule inhibitors (Blasius, 2011) (Fig. S1). Taken together, these analyses suggest that *Hydra* Chk1 is a potential target of SB 218078.

Given that the exposure of *Hydra* gastric segments to 5 μM of SB 218078 resulted in a distinct morphological phenotype, we examined the effects of SB 218078 on regeneration at both lower (3 μM) and higher (7 μM) concentrations. In general, the exposure of gastric segments to 3, 5 and 7 μM SB 218078 prevented regeneration and caused disintegration in both a dose- and time-dependent manner (Fig. 4). Additionally, the impact on regenera-

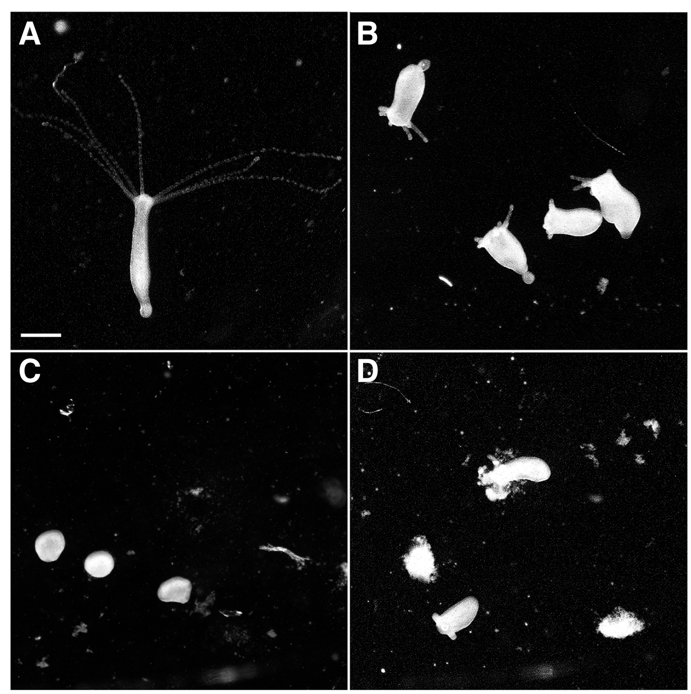

Fig. 2. Morphological categorization following exposure to the 80 kinase inhibitors. *In total, 4 major morphologies were observed in* Hydra *following exposure to the 80 kinase inhibitors:* **(A)** *complete regeneration,* **(B)** *partial regeneration – the presence of shortened tentacles and/or body column,* **(C)** *arrested regeneration - no formation of a head and foot, and* **(D)** *disintegration - the breakdown of tissues into debris. Scale bar in (A) represents 1000 µm and applies to all panels.*

tion was observed relatively early in the regeneration process: at 48 hours post exposure (hpe), control *Hydra* displayed at least 1 complete tentacle (80%) (Fig. 4A), while *Hydra* treated with 3, 5 and 7 μM appeared ball-shaped (Fig. 4 B-D).

Notably, *Hydra* head regeneration appeared to be more sensitive to SB 218078 exposure than regeneration of the foot. By 72 hpe, the majority of control *Hydra* displayed at least 4 complete tentacles (93%) and many formed a foot (40%) (Fig. 4E). In SB 218078-treated *Hydra*, while no tentacles or tentacle buds were observed (Fig. 4 F-H), 53% and 40% of *Hydra* in the 3 μM and 5 μM groups possessed a foot (Fig. 4 F-G). Additionally, disintegration begins to occur in the 7 μM group (Fig. 4H). By 96 hpe, complete head regeneration is observed in all control *Hydra* and the majority also possessed a foot (73%) (Fig. 4I). In contrast, disintegration is seen (to varying degrees) in all of the SB 218078-treated groups (Fig. 4 J-L), resulting in the greatest differences in regeneration scores compared to control *Hydra* (Fig. 4M). Moreover, *Hydra* treated with SB 218078 remain unable to regenerate complete head structures: few *Hydra* treated with 3 μM exhibited tentacle buds (20%) (Fig. 4J), while no tentacle-like formations are observed at the higher concentrations. However, foot regeneration was not inhibited to the same degree as head regeneration: complete foot structures were observed in some *Hydra* in the 3 μM (40%) and 5 μM treatment groups (20%) (Fig. 4 J-K). Taken together, these results show that the Chk1 inhibitor prevented regeneration and caused the loss of viability in a dose- and time-dependent manner. These trends are supported by the increasingly negative DEI values with both increasing concentration and exposure time (Fig. 4M). Furthermore, given that all SB 218078-treated *Hydra* were unable to form complete tentacle structures, head regeneration appears to be more sensitive to SB 218078 exposure than foot regeneration.

Exposure to SB 218078 disrupts* Hydra *head morphology and tentacle maintenance

As *Hydra* stem cells are constantly undergoing division and rapid turnover (Schenkelaars *et al.*, 2018), the *Hydra* model al-

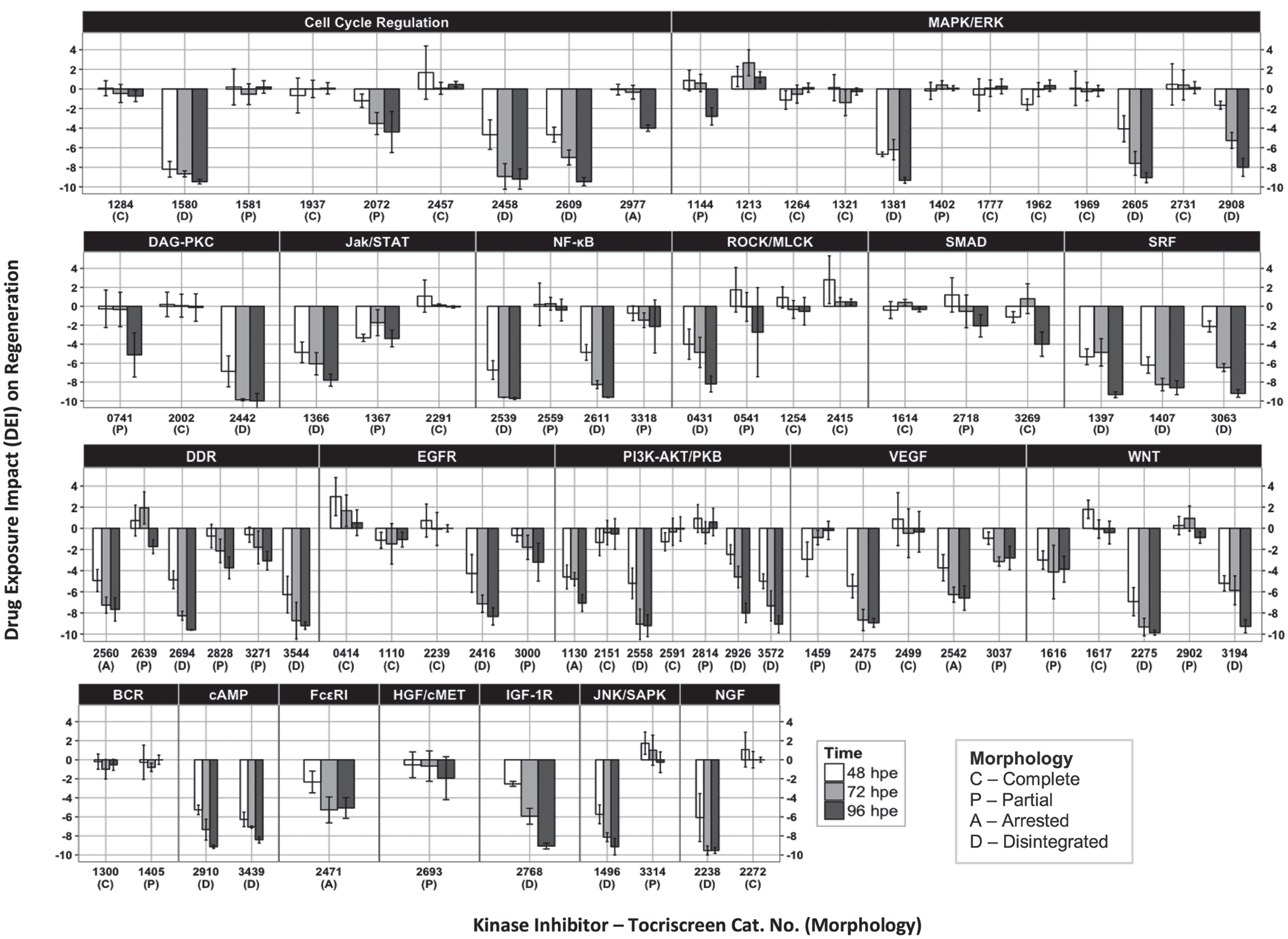

Fig. 3. Drug Exposure Impact of the 80 kinase inhibitors on *Hydra* regeneration. *Kinase inhibitors were grouped by the main signal transduction pathways they are presumed to target. Drug Exposure Impact (DEI) values on regeneration were calculated as the difference in regeneration scores obtained for control and* Hydra *exposed to 5 μM kinase inhibitor. DEI values for complete regeneration ranged between -1.07 and 1.2; partial regeneration ranged between -4.4 and 0.6; arrested regeneration ranged between -7.67 and -4; and disintegration ranged between -10 and -7.8. Error bars represent ± 2x standard error.*

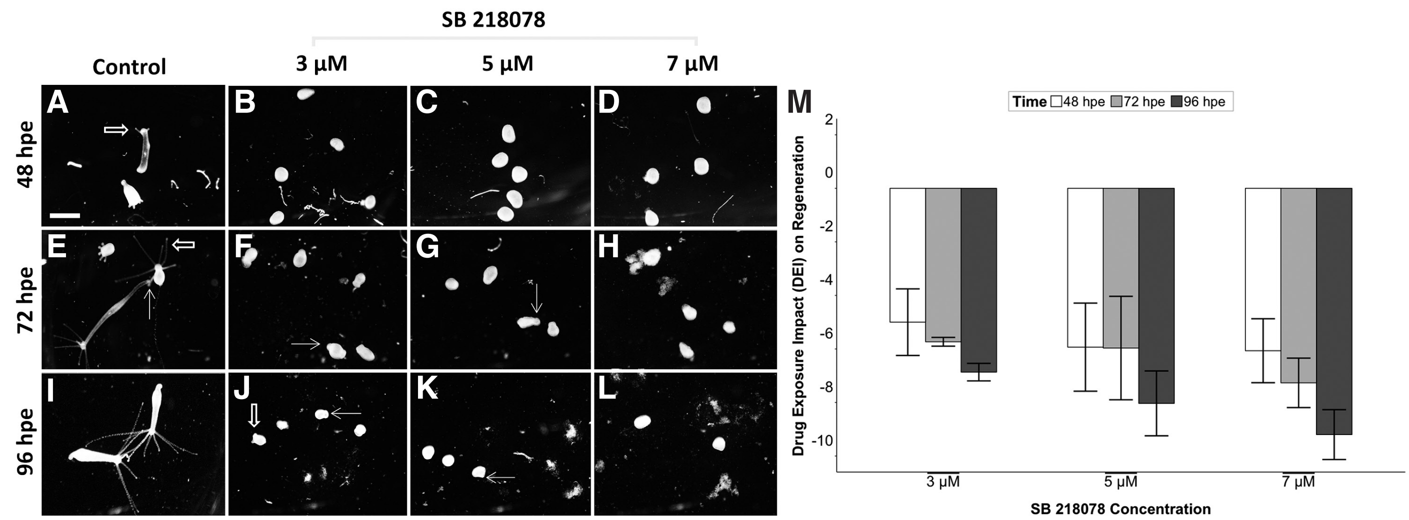

Fig. 4. Exposure to the Chk1 inhibitor SB 218078 prevents tentacle regeneration. Hydra *gastric segments were exposed to 3, 5, and 7 μM SB 218078 over a period of 96 hours.* Hydra *regeneration was scored using the Wilby 1988 classification scheme. At 48 hpe, control* Hydra *displayed tentacle formation* **(A)** *(marked by double arrow), while SB 218078-treated* Hydra *remained ball-shaped* **(B-D)**. *By 72 hpe, most control* Hydra *displayed d4 tentacles* **(E)** *(marked by double arrow), while SB 218078-treated* Hydra *lacked tentacle structures. Foot formation was detected in control* Hydra, *as well* Hydra *treated with 3 μM and 5 μM SB 218078* **(E-G)** *(marked by arrow). By 72 hpe,* Hydra *treated with 7 μM SB 218078 also begin to experience disintegration* **(H)**. *By 96 hpe, all control* Hydra *possessed p 4 tentacles and many showed a foot* **(I)**. *Complete tentacle regeneration was not seen in SB 218078-treated groups, tentacle buds were detected in 3 μM SB 218078-treated* Hydra **(J)** *(marked by double arrow). Moreover, foot regeneration was not disrupted in* Hydra *treated with 3 μM and 5 μM SB 218078* **(J-K)** *(marked by arrow). Drug Exposure Impact (DEI) values on morphology were calculated as the difference in morphology scores obtained for control and* Hydra *exposed to 1, 2 and 3 μM SB 218078* **(M)**. *By 96 hpe, disintegration was seen (in varying degrees) in all of the SB 218078-treated groups* **(J-L)**, *resulting in the largest negative DEI values on regeneration* **(M)**. *Error bars represent ± 2x standard error. Scale bar in (A) represents 1000 μm and applies to all panels.*

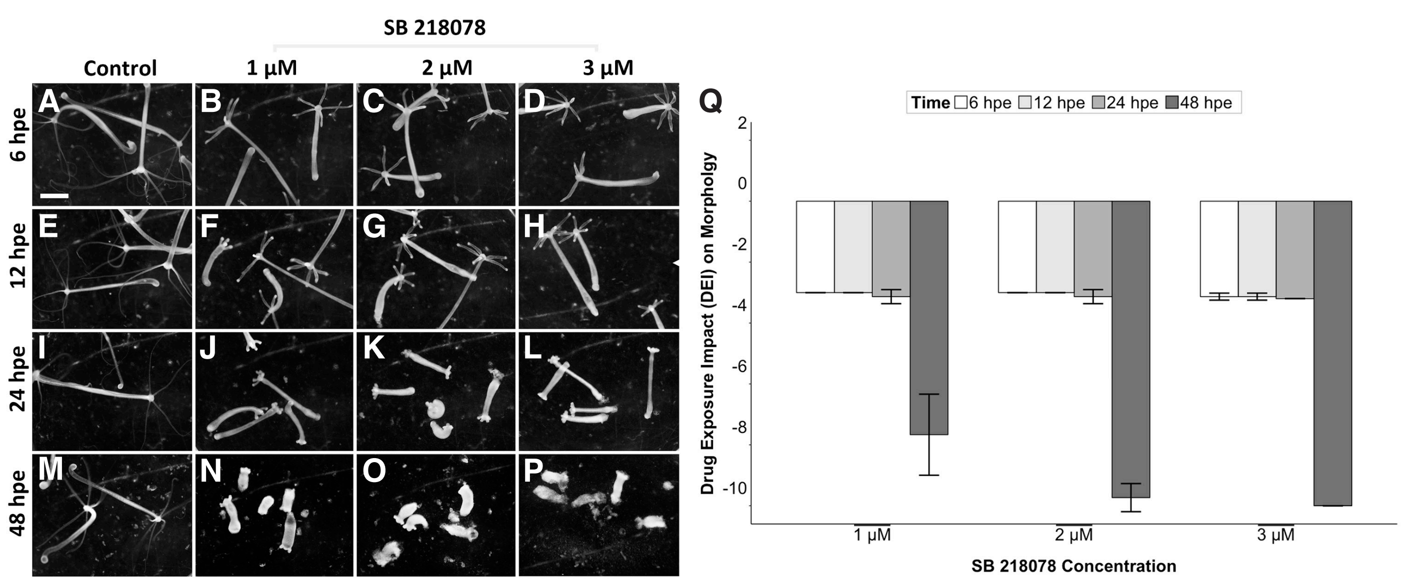

Fig. 5. Exposure to the Chk1 inhibitor SB 218078 causes shortening and eventual loss of tentacles. *Intact* Hydra *were treated with 1, 2, and 3 μM SB 218078 over a period of 48 hours.* Hydra *morphology was scored using the Wilby 1988 classification scheme. Control* Hydra *maintained elongated tentacles and body columns throughout the exposure* **(A,E,I,M)**, *while SB 218078-treated* Hydra *exhibited tentacle shortening by 6 hpe* **(B-D)**, *clubbed tentacles by 12 hpe* **(F-H)**, *bud-like tentacles and shortened body columns by 24 hpe* **(J-L)** *and further shortening or disintegration by 48 hpe* **(N-P)**. *Drug Exposure Impact (DEI) values on morphology were calculated as the difference in morphology scores obtained for control and* Hydra *exposed to 1, 2 and 3 μM SB 218078* **(Q)**. *By 48 hpe, disintegration is seen (in varying degrees) in all of the SB 218078-treated groups* **(N-P)**, *resulting in the largest negative DEI values on morphology* **(Q)**. *Error bars represent ± 2x standard error. Images were taken with the Leica M165 scope and Leica Application Suite software. Scale bar in (A) represents 1000 μm and applies to all panels.*

Fig. 6. Exposure to the Chk1 inhibitor SB 218078 does not disrupt the foot specific of expression of peroxidase. Hydra *exposed to 1 μM SB 218078 for 12 and 24 hours were stained for peroxidase activity, a proxy for foot specific differentiation. The pattern of peroxidase activity in control* **(A, C)** *and SB 218078-treated* Hydra **(B,D)** *were indistinguishable indicating that exposure to this Chk1 inhibitor did not affect foot maintenance. In contrast, the tentacles of* Hydra *exposed to SB 218078 are dramatically shortened at 12 hpe* **(B)**, *and bud-like or non-detectable by 24 hpe* **(D)**. *Scale bar in (A) represents 1000 μm and applies to all panels.*

lows for the simultaneous study of both self-renewal and normal physiology. Since SB 218078-treated *Hydra* displayed a differential sensitivity in terms of head and foot regeneration, we became interested in the effects of the Chk1 inhibitor on intact *Hydra*. Given that the previous SB 218078 concentrations resulted in dramatic morphological effects and the loss of viability over time, we decided to test lower concentrations of 1, 2 and 3 μM. Intact *Hydra* were exposed to these various SB 218078 concentrations for a period of 48 hours, and the morphology of each animal was scored. In general, exposure to 1, 2 and 3 μM SB 218078 resulted in the gradual shortening of *Hydra* tentacles and body columns over time. While control *Hydra* possessed elongated tentacles and body columns throughout the entire experiment (Fig. 5 A, E, I, M), SB 218078-treated *Hydra* displayed shortened tentacles by 6 hpe (Fig. 5 B-D), clubbed tentacles by 12 hpe (Fig. 5 F-H), bud-like tentacles and shortened body columns by 24 hpe (Fig. 5 J-L), and further shortening or disintegration by 48 hpe (Fig. 5 N-P). However, this time-dependent impact on morphology was not depicted in the DEI values (Fig. 5Q) since the Wilby 1988 classification scheme does not consider the varying degrees of tentacle and body shortening (Quinn *et al*., 2012). With respect to the dose-dependent effects, *Hydra* morphology amongst the various SB 218078 concentrations were indistinguishable at the earlier time points (Fig. 5 B-D, F-H, J-L); this is represented by the relatively similar DEI values between the concentrations from 6-24 hpe (Fig. 5Q). However, by 48 hpe, the number of disintegrated *Hydra* increased with increasing concentrations (Fig. 5 N-P), which is shown by the increasingly negative DEI values at this time point (Fig. 5Q).

The *Hydra* basal disc is comprised of epithelial-derived mucous cells containing a peroxidase-like enzyme, which allows for the detection of foot-specific differentiation. *Hydra* stained with diaminobenzidine results in a dark-brown colour within the cells containing the peroxidase activity (Hoffmeister and Schaller, 1985). To confirm foot differentiation in *Hydra* exposed to the Chk1 inhibitor, we stained intact animals with diaminobenzidine immediately following exposure to 1 μM SB 218078 for 12 and 24 hours. *Hydra* exposed to SB 218078 exhibited a strong dark brown staining at the basal end, similar to their respective controls (Fig. 6). Together with the above data, it is suggested that Chk1 inhibitor-exposed *Hydra* had no apparent disruptions in foot differentiation.

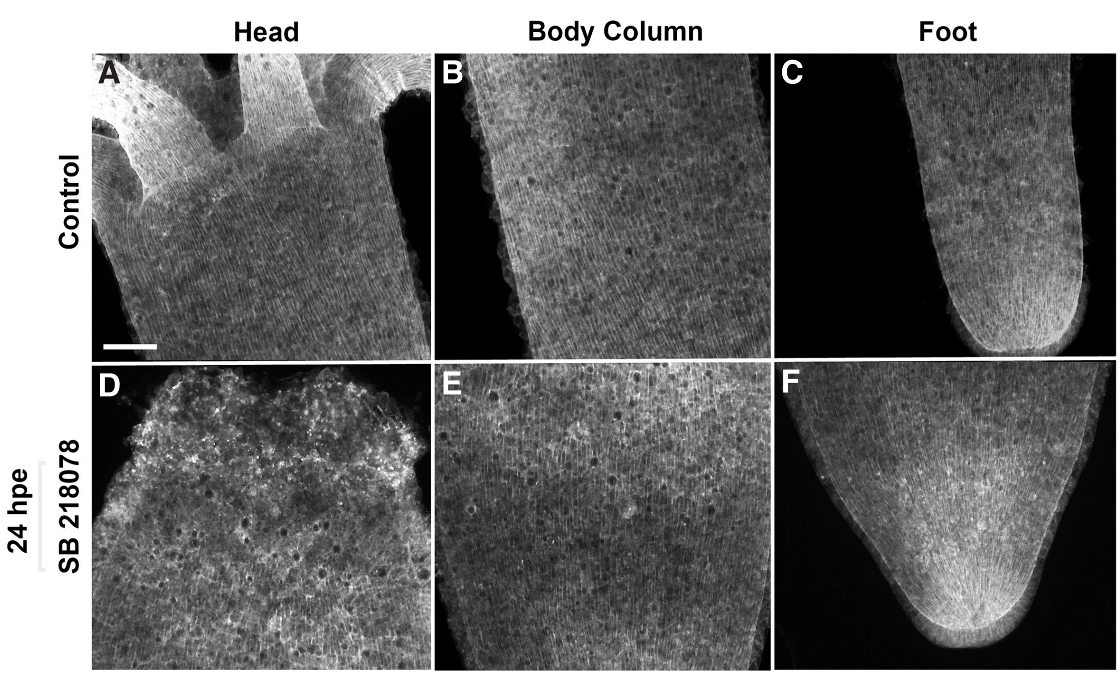

Fig. 7. Exposure to the Chk1 inhibitor SB 218078 results in F-actin disorganization in the *Hydra* head region. Hydra *exposed to 1 μM SB 218078 for 24 hours were stained with rhodamine conjugated phalloidin in order to visualize the F-actin structures. Control* Hydra *displayed long, continuous filaments along the oral aboral axis* **(A-C)**, *while SB 218078-treated* Hydra *exhibited disorganized F-actin only in the head region seen here with much reduced tentacles* **(D,E,F)**. *Scale bar in (A) represents 100 μm and applies to all panels.*

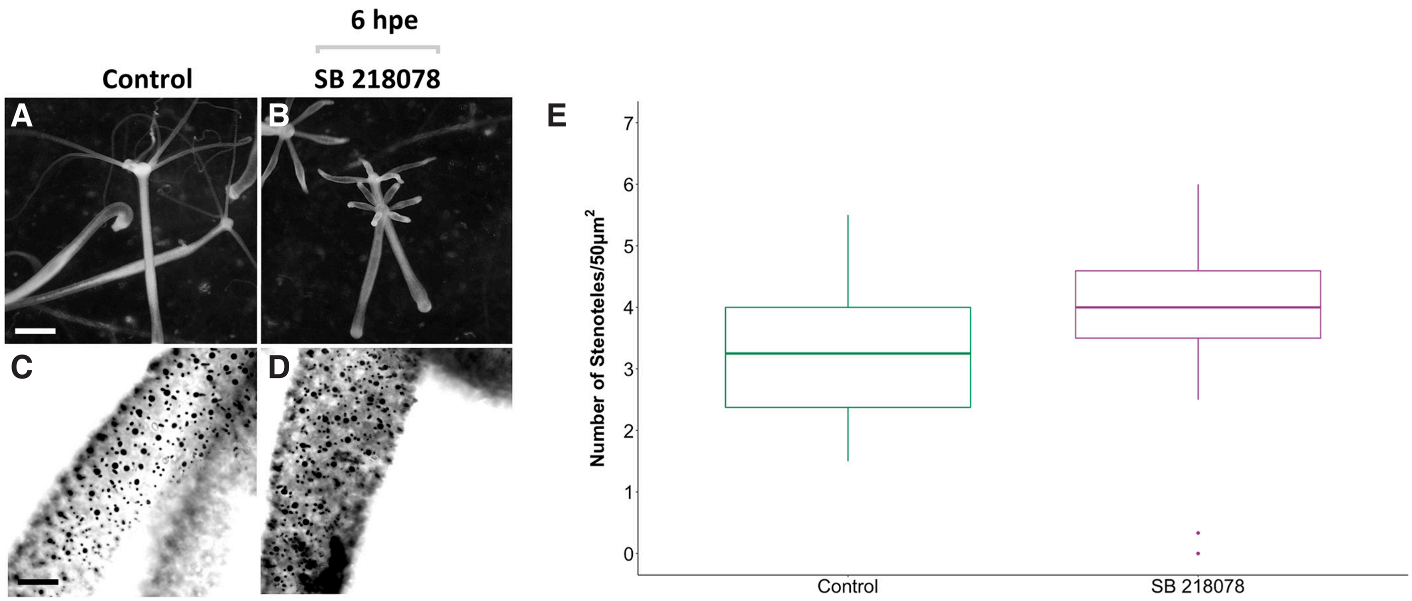

Fig. 8. Exposure to the Chk1 inhibitor SB 218078 does not appear to impact the density of stenoteles and the overall organization of the nematocytes in the battery cell complex. Hydra *exposed to 1 µM SB 218078 for 6 hours were stained with toluidine blue to detect the stenotele nematocysts. Panels* **(A)** *and* **(B)** *display the overall morphology of control and SB 218078-treated* Hydra*, respectively. Reduction in the overall length of the tentacles is already apparent at this time. Panels* **(C)** *and* **(D)** *display toluidine blue stained control and SB 218078-treated tentacles, respectively. The overall organization of the nematocytes seen here by toluidine blue staining of the nematocyst organelle does not appear to be affected by exposure to the Chk1 inhibitor SB 218078. The number of stenoteles in the proximal region of tentacles were counted manually and density was determined per 50 µm² fields. No significant difference in stenotele density was detected between control and SB 218078-treated* Hydra **(E)**. *Scale bar in (A) represents 1000 µm and also applies to (B). Scale bar in (C) represents 50 µm and also applies to (D).*

Actin organization is crucial for *Hydra* morphogenesis and regeneration (Livshits *et al.,* 2017). Thus, we hypothesized possible discrepancies in actin fiber alignment in *Hydra* treated with SB 218078. To test this, intact *Hydra* treated with 1 µM SB 218078 for 24 hours were stained with rhodamine-phalloidin to visualize the F-actin structures. While control *Hydra* displayed long, continuous filaments throughout the whole animal (Fig. 7 A-C), SB 218078-treated *Hydra* showed disorganized filaments in the head region (Fig. 7D). However, F-actin structure in the body column and foot resembled those of control animals (Fig. 7 E-F). Taken together, these findings suggest that SB 218078 predominantly disrupts *Hydra* head morphology, contributing to its inability to maintain tentacle structures.

Since *Hydra* exposed to 1 µM SB 218078 displayed shortened tentacles as early as 6 hpe (Fig. 8 A-B), we examined the cellular components within the tentacles, specifically those involved in feeding functions. *Hydra* tentacles are normally constituted of battery cells that are epitheliomuscular cells embedded with numerous nematocysts that are responsible for prey capture (Hufnagel *et al.,* 1985). We focused on stenotele nematocysts since they are easily distinguished by their large size. To this end, *Hydra* exposed to 1 µM SB 218078 for 6 hours were stained with toluidine blue and the stenoteles in the proximal tentacle regions were counted (Fig. 8 C-D). We examined the proximal areas since the medial and distal portions were easily tangled during the staining process. No significant difference in stenotele density was detected between control and SB 218078-treated *Hydra* (Fig. 8E). These results indicate that although the Chk1 inhibitor disrupts the overall morphology of the tentacles, select components inside the tentacular epithelial cells appear to be unchanged.

Exposure to SB 218078 alters cellular composition of the Hydra *gastric region*

Hydra epithelial cells are constantly being displaced from the gastric zone to the apical and basal extremities, differentiating into either tentacle- or foot-specific cells (Schenkelaars *et al.*, 2018). Given the gradual loss of tentacles structures in SB 218078-treated *Hydra*, we decided to investigate the cellular composition of the body column. *Hydra* exposed to 1µM SB 218078 for 12 and 24 hours were dissected to isolate the gastric region, subsequently macerated, and the various cell types were counted: ectodermal epithelial, endodermal epithelial, interstitial, nematoblasts, nematocysts, gland, and nerve cells (Fig. 9A). Notably, *Hydra* treated with SB 218078 revealed significantly lower proportions of ectodermal epithelial cells compared to their controls at both 12 and 24 hours; and significantly lower proportions of endodermal epithelial cells at 24 hours (Fig. 9B). The remaining cell type proportions were comparable between SB 218078-treated and control *Hydra* at both time points. These results correspond to the unchanged stenotele density observed in SB 218078-treated *Hydra* at 6 hpe, given that nematocysts are derived from nematoblasts and interstitial cells, and no changes in proportions were seen in any of these cell types. Overall, these results indicate that the Chk1 inhibitor primarily impacts the *Hydra* epithelial stem cells, which may account for its overall poor tentacle maintenance.

Changes in Hydra *cellular composition caused by exposure to SB 218078 is not accompanied by alterations in mitotic or apoptotic activities*

Disruptions in the G2/M cell cycle checkpoint may allow a damaged cell to enter pre-mature mitosis and subsequently apoptotic cell death (DiPaola, 2002). The mitotic and apoptotic activities of SB 218078-treated *Hydra* were investigated, as changes in these cellular processes may account for its poor regeneration, disrupted tentacle maintenance and reduced epithelial cell proportions. First, we performed a phospho-histone H3 antibody assay to detect mitotically active cells. *Hydra* treated with 1μM SB 218078 for 12 and 24 hours were stained with anti-phosphorylated histone H3 and the fluorescent nuclei in the body column were manually counted (Fig. 10 A-D). DAPI was used to verify that the fluorescence signal from anti-phosphorylated histone H3 were indeed nuclei (Fig. 10 E-F). The average fluorescent nuclei density (fluorescent nuclei/μm^2) in *Hydra* exposed to 1μM SB 218078 at both 12 and 24 hours were not significantly different to their corresponding control groups (Fig. 10G). Next, SB 218078-treated *Hydra* were stained with acridine orange to detect possible changes in apoptotic activity (Fig. 11 A-D). Similarly, acridine orange fluorescence intensity (a.u) of *Hydra* exposed to 1μM SB 218078 for 12 hours and 24 hours were not significantly different to their corresponding control groups (Fig. 11E). Taken together, these results indicate that reduced epithelial cell proportions in SB 218078-treated *Hydra* are not due to major changes in cell division or apoptotic cell death.

Discussion

To date, the molecular basis of tissue regeneration and wound repair is not fully understood, consequently limiting the development of novel clinical strategies in regenerative medicine (Eming *et al.,* 2016). Interestingly, cross-phyla studies within the animal kingdom have demonstrated that regeneration maintains an extensive conservation of molecular signaling pathways (Alvarado and Tsonis, 2006). For this reason, the study of animals that exhibit robust regeneration, such as *Hydra*, may improve our knowledge of the key regulators and mechanisms driving adult tissue repair and wound healing. Many studies have utilized kinase inhibitors to identify molecular regulators and signal transduction pathways underlying *Hydra* regeneration and patterning (Cardenas *et al.*, 2000; Cardenas and Salgado, 2003; Broun *et al.,* 2005; Manuel *et al.*, 2006; Arvizu *et al.*, 2006; Turwankar and Ghaskadbi, 2019). In the present study, we describe a systematic screen of a kinase inhibitor library to investigate their effects on *Hydra* regeneration. We focused on SB 218078, a potent inhibitor of Chk1, considering its crucial role in the G2/M checkpoint and the importance of G2-paused cells in *Hydra* regeneration.

We found that *Hydra* that had been exposed to the Chk1 inhibitor SB 218078 were incapable of head-specific regeneration and maintenance. Specifically, *Hydra* gastric segments exposed to SB 218078 were unable to regenerate complete tentacle structures; while foot regeneration was seen in *Hydra* exposed to lower con-

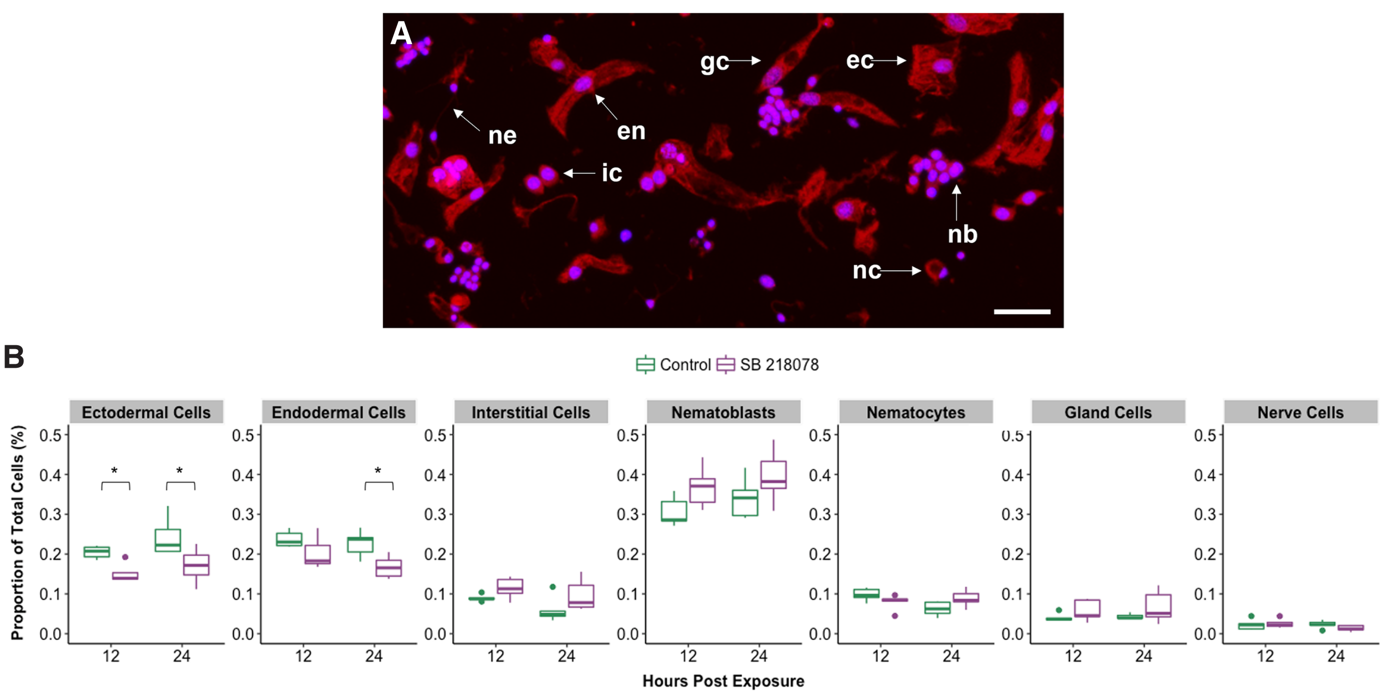

Fig. 9. Exposure to the Chk1 inhibitor SB 218078 leads to reduction in the relative proportion of epithelial cells in the gastric region. *Cell macerates from* Hydra *exposed to 1 μM SB 218078 for 12 and 24 hours were stained with Mitotracker and DAPI to visualize the mitochondria and nuclei. Panel* **(A)** *shows a representative photomicrograph from a control cell macerate with the cell types counted in this experiment (ec - ectodermal epithelial cells; en - endodermal epithelial cells; ic - interstitial cells; nb - nematoblasts; nc - nematocysts; gc - gland cells; ne - nerve cells). For each treatment group, 627 – 1333 cells were counted to determine the relative proportion of the various cell types.* **(B)** Hydra *exposed to SB 218078 had significantly lower proportion of ectodermal epithelial cells compared to control at both 12 and 24 hours; and significantly lower proportions of endodermal epithelial cells at 24 hours. Asterisks indicate significant differences (p<0.05). Scale bar in (A) represents 100 μm.*

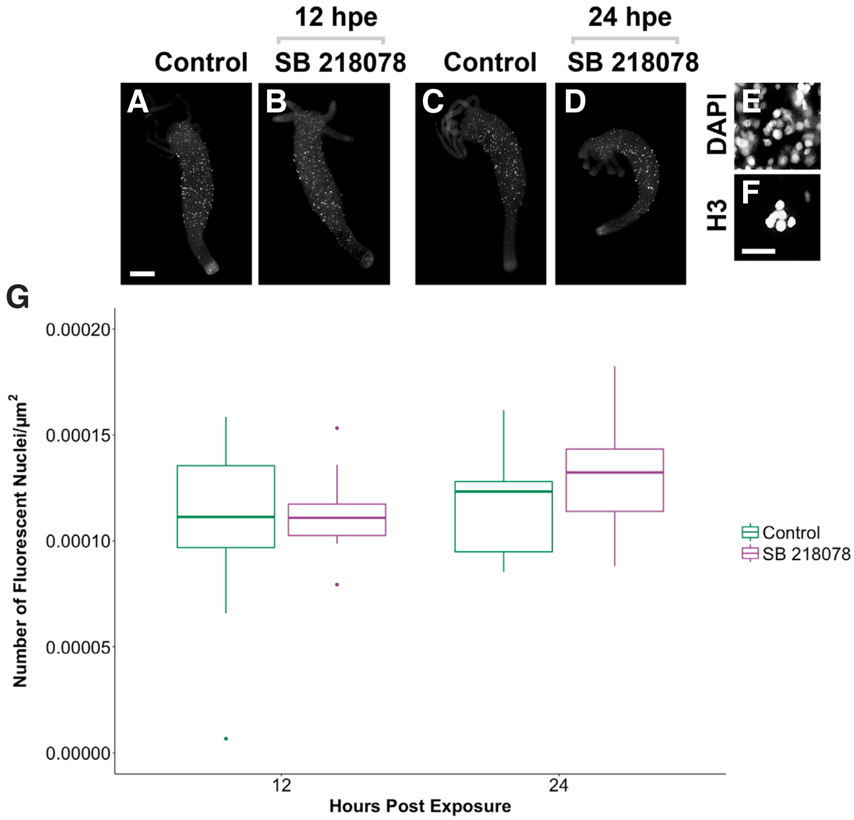

Fig. 10. Exposure to the Chk1 inhibitor SB 218078 does not impact mitotic activity in the *Hydra* gastric region as detected by anti-phosphorylated histone H3 immunolabelling. Hydra *exposed to 1 µM SB 218078 for 12 and 24 were processed for anti-phosphorylated histone H3 immunolabeling to detect mitotically-active nuclei.* **(A)** *and* **(C)** *display non-exposed control* Hydra *at 12 and 24 hpe, respectively;* **(B)** *and* **(D)** *represent SB 218078-exposed* Hydra *at 12 and 24 hpe, respectively;* **(E)** *and* **(F)** *show the overlap of anti-phosphorylated histone H3 labelling and DAPI indicating that the structures detected with the anti-phosphorylated histone H3 antibody are indeed nuclei. The number of fluorescent nuclei in the entire animal (excluding the tentacles) were counted manually to determine the density (fluorescent nuclei/µm²). No significant differences in fluorescent nuclei density were found between the treatment groups at 12 or 24 hpe* **(G)**. *Images were taken with the Axio Observer D1 scope and ZEN Blue software. Scale bar in (A) represents 500 µm and also applies to (B-D). Scale bar in (F) represents 25 µm and also applies to (E).*

centration of the inhibitor. Likewise, intact *Hydra* exposed to SB 218078 experienced a gradual shortening and eventual loss of tentacles; while foot structures appeared unchanged. In line with these observations, *Hydra* exposed to SB 218078 for 24 hours displayed disorganized actin filament structure in the head region, below the tentacles, but not in the foot region. Notably, SB 218078 treated *Hydra* had a significantly lower proportion of ectodermal epithelial cells compared to their controls at both 12 and 24 hours; and significantly lower proportion of endodermal epithelial cells at 24 hours. In contrast, no differences were seen for interstitial stem cells or their derivatives. This finding is consistent with the observation that exposure to SB 218078 did not affect the tentacle density of stenoteles; a specialized nematocyte derived from the multipotent interstitial stem cell. Lastly, exposure to SB 218078 appeared to have no impact on the level of mitosis or apoptosis as detected by anti-phospho H3 immuno-labelling and acridine orange respectively and under the conditions employed in our experiments.

Axial patterning in *Hydra* is largely determined by the morphogenetic gradients termed the head activation (HA) and head inhibition (HI) gradient; both signals originate from the head organizer, located in the hypostome, and decrease in concentration down the body column (Bode, 2009). In addition to these morphogenetic patterns, *Hydra* head and foot regeneration are associated with different signaling pathways; inhibition of Src tyrosine kinase, ERK 1–2, PI3K, MEK, and ribosomal S6 kinase (RSK) disrupts *Hydra* head but not foot regeneration (Galliot, 2013). Furthermore, phosphorylation patterns during head regeneration are different from foot regeneration: cAMP-response element-binding protein (CREB) is hyperphosphorylated in the regenerating head stumps; in the basal region, there are higher levels of phosphorylated Smad, indicating greater BMP signaling activity (Kaloulis *et al.*, 2004; Wenger *et al.*, 2019). Lastly, head and foot regeneration are different in terms of their cellular events. At the head-regenerating tips, there is an immediate wave of cell death promoting regeneration, however, this is not seen for the foot (Chera *et al.*, 2009). Collectively, these studies indicate that *Hydra* head and foot regeneration are independent processes. In the present work, we show that *Hydra* head regeneration is more sensitive to SB 218078 treatment, suggesting a potential role for *Hydra* Chk1 in the regeneration of head-specific processes.

In *Hydra*, epithelial stem cells generated in the body column are progressively displaced bidirectionally towards the oral aboral extremities. Once there, both ectodermal and endodermal epithelial cells stop cycling and undergo a tentacle or foot specific differentiation program. Tentacle and foot epithelial cells will eventually be shed into the media and new cells will differentiate and be incorporated in these structures (Bosch, 2007). Therefore, continuous cell shedding at the tentacles and foot is balanced by the differentiation of epithelial stem cells that by virtue of their continuous proliferation are displaced from the gastric column to the apical extremities. Interestingly, early experiments indicate that the displacement of epithelial cells from the base of the tentacle into the tentacle proper occurs much faster than that of epithelial cells into the basal disc or foot region (4 days versus 20 days) (Campbell, 1967). Taken together, these observations suggest that the turnover of tentacle epithelial cells is higher than that of foot epithelial cells. It is thus possible that the differential sensitivity of intact *Hydra* to SB 218078 observed along the oral-aboral axis reflects the higher turnover

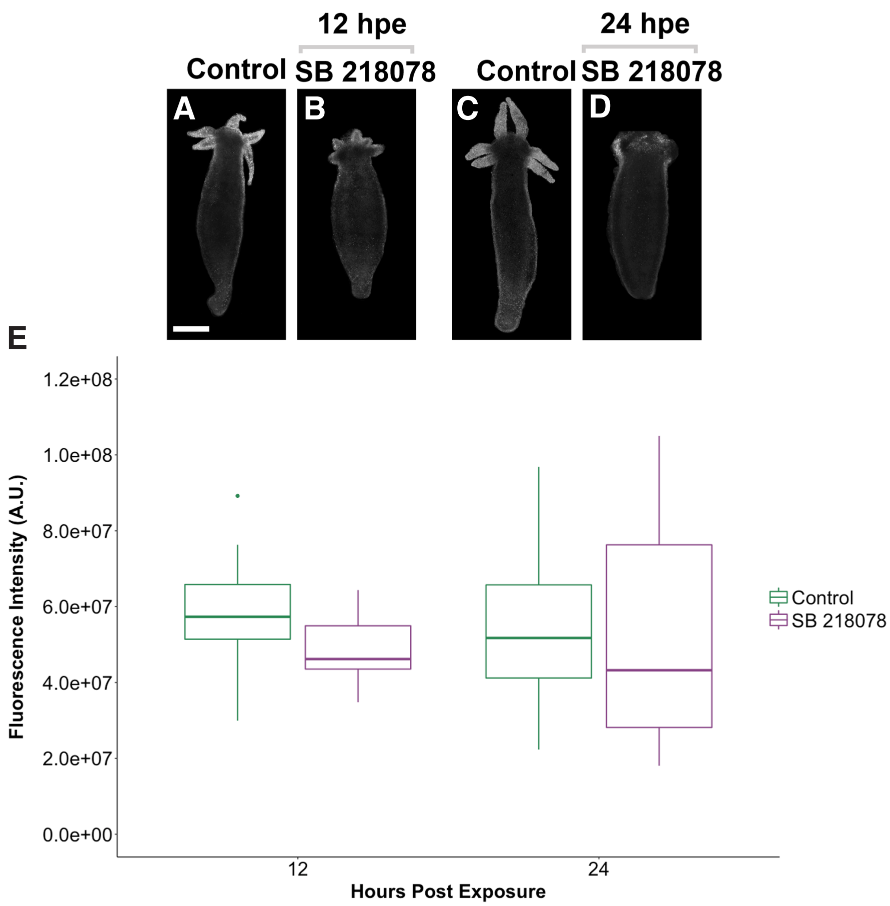

Fig. 11. Exposure to the Chk1 inhibitor SB 218078 does not increase apoptosis in the *Hydra* gastric region. Hydra *exposed to 1 μM SB 218078 for 12 and 24 hours were stained with acridine orange to detect apoptotic cells. Panels* **(A)** *and* **(C)** *show control* Hydra *at 12 and 24 hpe, respectively; panels* **(B)** *and* **(D)** *show SB 218078-treated* Hydra *at 12 and 24 hpe, respectively. Fluorescence intensity in the entire animal, excluding the tentacles, was measured using ImageJ. No significant difference was found between the treatment groups at 12 or 24 hpe* **(E)**. *Images were taken with the Axio Observer D1 scope and ZEN Blue software. Scale bar in (A) represents 500 μm and applies to all panels.*

of the tentacle structure. Alternatively, exposure to SB 218078 may cause a relative increased loss of tentacle structures due to disruption of the cell shedding processes. In the mammalian intestine, F-actin organization is thought to be important in facilitating the shedding of epithelial cells. Specifically, dying epithelial cells are squeezed out of the epithelium by the contraction of an actin myosin ring (Wang *et al.,* 2011). In our results, we found that SB 218078-treated *Hydra* showed disorganized actin filament structure in the head region immediately at the base of the tentacles, but not in the body column or foot region. Thus, this head-specific actin disruption may have resulted in reduced incorporation or differentiation of epithelial cells into the tentacles, as reflected in the shortened and stubby appearance of tentacles.

At the level of resolution investigated here, SB 218078 exposure reduced the relative proportion of epithelial stem cells without affecting interstitial stem cells and derivatives (nematoblasts, nematocytes, gland cells, nerve cells). It is possible that this differential impact to SB 218078 exposure is due to longer cell cycle duration of epithelial cells (3-4 days) relative to that reported for interstitial stem cells (24-30 hours) (Hobmayer *et al.*, 2012; Buzgariu *et al.*, 2014). *Hydra* regeneration can occur in the so-called epithelial *Hydra* nearly devoid of interstitial stem cells and derivatives (Marcum and Campbell, 1978; Sugiyama and Fujisawa, 1978). However, disruptions in the ability of epithelial stem cells to proliferate can drastically limit *Hydra* regenerative potential (Bosch, 2007), which appeared to be consistent with our results.

In *Hydra*, head regeneration has been shown to rely on large numbers of G2-paused adult stem cells (Buzgariu *et al.,* 2018). *Hydra* head regeneration following decapitation has been suggested to be a largely morphallactic process which depends on the differentiation of existing epithelial stem cells. In fact, it has been indicated that head-specific differentiation can occur in the absence of cellular proliferation, possibly as an adaptive mechanism (Buzgariu *et al.*, 2018). Furthermore, the ectodermal epithelial cells of the *Hydra* tentacles (known as battery cells) and the foot (known as foot mucous cells) possess 4n DNA content (Dubel *et al.,* 1987). Taken together, it is indicated that battery and foot mucous cells are G2-arrested and have been terminally differentiated in a single step.

Chk1 was first identified in fission yeast as a serine threonine kinase that controls G2/M transition in response to DNA damage (Walworth *et al.,* 1993). As a checkpoint protein, Chk1 negatively regulates G2/M transition. Increased activity of Chk1 holds cells in G2 phase. Activated Chk1 phosphorylates several different targets triggering a cascade of cellular processes that include cell cycle arrest or delay, DNA repair and on the extent of the DNA damage present, apoptosis (Zhang and Hunter, 2014). In addition, Chk1 plays a role in monitoring DNA replication. Inhibition or downregulation of Chk1 may lead to so-called mitotic catastrophe due to cells with incomplete replication entering mitosis prematurely. A role for Chk1 function in normal cell growth is mediated by phosphorylation events distinct from those mediating the DNA damage response. Mutational analysis indicates that the DNA damage response function of Chk1 dependent on phosphorylation of S317 residue is non-essential. In contrast, cell cycle regulation mediated by phosphorylation of S345 is essential for cell viability and has been proposed to promote progression to metaphase (Wilsker *et al.,* 2008). Consistent with these findings, downregulation of Chk1 in synchronized cells blocks cell cycle at metaphase (Tang *et al.*, 2006).

In general, stem cell differentiation is primarily associated with the length of the G1 phase. Indeed, manipulation of genes known to promote G1 length, particularly cdk2/cyclin E, is capable of influencing embryonic stem cell (ESCs) differentiation (Lange and Calegari, 2010). However, the link between G2 cell cycle pausing and differentiation has been demonstrated in human

ESCs. Specifically, the disruption of Wee1-mediated G2 pausing in hESCs selectively reduced early lineage commitment to endoderm (Van Oudenove *et al*., 2016). The importance of G2 in stem cell differentiation is consistent with the postulation of Chk1's role in this process. In particular, treatment of CD133+ hematopoietic stem cells (HSC) with Chk1 inhibitors led to a decrease in myeloid precursor percentage, and an increase in lymphoid precursor percentage, suggesting a possible role of Chk1 in HSC differentiation (Carrassa *et al.,* 2010). Moreover, loss of Chk1 has been associated with an inhibition of T lineage differentiation in thymocytes (Zaugg *et al.,* 2007). Taken together, we postulate that Chk1 inhibitor-exposed *Hydra* may have defects in apical differentiation, contributing to their apparent inability to regenerate or maintain tentacles. Specifically, there may be disruptions in the terminal differentiation of epithelial stem cells to tentacle-specific battery cells. Considering there were no changes in the proportions of interstitial-derived cells in the gastric column or tentacles of SB 218078-treated *Hydra*, Chk1 may not impact the differentiation of interstitial stem cells.

G2 pausing has been proposed to assist in the protection against cell death (Buzgariu *et al.,* 2014). Specifically, most cells in the G2 phase resist pro-apoptotic agents, while cells cycling in the G1 or S-phases rapidly undergo cell death (Reiter *et al.,* 2012). Furthermore, human epithelial cells with stem-like properties are able to resist cell death in G2, due to increased levels of Chk1 and Chk2 proteins (Harper *et al.,* 2010). In our study, gastric columns of SB 218078-treated *Hydra* displayed no detectable changes in apoptotic activity, as shown by acridine orange staining. In the future, SB 218078-treated *Hydra* should be exposed to apoptosis-inducing agents such as colchicine or wortmannin to evaluate their resilience against cell death. Our results suggest that the baseline level of apoptotic cell death in *Hydra* is not affected by exposure to Chk1 inhibitor. It is possible that higher levels of apoptosis are occurring in the tentacles of SB 218078-treated *Hydra*; however, this is obscured by the affinity of acridine orange to poly-γ -glutamate in nematocyst capsules. Thus, it would be worthwhile checking for programmed cell death in the tentacles using other apoptosis-detection assays such as terminal deoxynucleotidyl transferase (TdT) dUTP Nick-End Labeling (TUNEL).

Overall, our study demonstrates the effectiveness of kinase inhibitor screens for investigating key regulators of *Hydra* regenerative processes. We determined that SB 218078, a Chk1 inhibitor, disrupts the head region in both regenerating and intact *Hydra*. Although molecular and biochemical assays are necessary to determine the specific targets of SB 218078 in *Hydra*, our findings suggest a potential role for Chk1 in head-specific regeneration and maintenance.

Materials and Methods

Maintenance of Hydra *cultures*

Hydra vulgaris (synonym *H. littoralis*) were obtained from Ward's Natural Science Ltd (Rochester, New York). *Hydra* cultures were kept in glass Pyrex dishes (8 x 8 x 1.5 inch) containing 600 ml of *Hydra* medium (HM). HM was made fresh weekly by dissolving 0.5M $CaCl_2$, 0.5 M NaCl, 0.5 M KCl, 0.05 M $MgSO_4$ and 0.5 M Tris Base into distilled water, which was then adjusted to a pH of 7.7. The cultures were maintained at 12/12 h light-dark photoperiod at a temperature of 22°C. *Hydra* were fed on the weekdays with *Artemia nauplii* and the HM was replaced with fresh solution approximately six hours after feeding.

Kinase inhibitor screen on regeneration

A panel of 80 kinase inhibitors (Tocriscreen Kinase Inhibitor Toolbox Cat. No. 3514) dissolved as 10 mM solutions in dimethyl sulfoxide (DMSO) was obtained from Tocris Bioscience (Bristol, United Kingdom). *Hydra* gastric segments were isolated by cutting starved (1-day) specimens with a scalpel immediately below the head and immediately above the basal disc. Three kinase inhibitors (5 μM) and one control (HM with 0.05% DMSO) were set up per 12-well plate: three replicate wells for each treatment group with 5 *Hydra* gastric segments/well. Each well contained 3 ml of the appropriate treatment solution (Fig. 1). Regeneration was scored for each specimen every 12 hours for 4 days using the Wilby 1988 classification chart of *Hydra* regeneration (Quinn *et al*., 2012). This grading system consists of assigning a score between 0 – 10 for each individual *Hydra*, with a score of 10 indicating complete regeneration of the head and foot, while a score of 0 represents disintegration and a lack of regeneration. Additionally, the overall morphology of each *Hydra* was noted at the end of the 96-hour exposure. The drug exposure impact (DEI) value for regeneration was calculated by subtracting the mean regeneration score for the vehicle-treated control group from the mean regeneration score for the inhibitor-treated group. Throughout the exposure, *Hydra* were not fed, and the solution was not replaced. Specimens were imaged with the Leica M165 dissecting scope and Leica Application Imaging Suite software.

Morphology assay

Whole *Hydra* were distributed into 3 wells (5 *Hydra*/well) containing 3 ml of a given concentration of SB 218078 or DMSO vehicle control. The impact of kinase inhibitors on *Hydra* viability was assessed using the Wilby 1988 classification chart of *Hydra* morphology (Quinn *et al*., 2012). This grading system consists of assigning a score between 0 – 10 for each *Hydra*, with a score of 10 indicating extended tentacles and a reactive body, while a score of 0 represents disintegration. The DEI value for morphology was calculated by subtracting the mean morphology score for the vehicle-treated control group from the mean morphology score for the inhibitor-treated group. Throughout the exposure, *Hydra* were not fed, and the solution was not replaced. Specimens were imaged with the Leica M165 dissecting scope and Leica Application Imaging Suite software.

Visualization of filamentous actin with rhodamine-phalloidin

Hydra exposed to 1 μM SB 218078 (Tocris) for 24 hours were stained with rhodamine conjugated phalloidin to visualize F-actin structures. Rhodamine-phalloidin staining was carried out as previously described (Aufschnaiter *et al.,* 2017). Briefly, *Hydra* were relaxed in 2% urethane/HM for 2 min, fixed in 4% paraformaldehyde/HM at 4°C for 1 hour, washed 3× in 1X PBS for 10 min, then permeabilized with 0.1% Triton/PBS for 15 minutes at room temperature. After permeabilization, *Hydra* were incubated in Alexa Fluor 488 Phalloidin (1:200) (Thermo Fisher) in 0.1% Triton/PBS for 1 hour at room temperature, washed 3× in 1X PBS for 10 min, then mounted with Mowiol 4-88 (Sigma). Specimens were imaged with the Zeiss AXIO Observer D1 microscope and ZEN software. Sample size: N=15 for inhibitor-treated *Hydra* at 24 hpe; N=14 for control *Hydra*.

Anti-phosphorylated histone H3 immunolabelling

Hydra exposed to 1 μM SB 218078 (Tocris) for 12 and 24 were processed for anti-phosphorylated histone H3 immunolabeling to detect mitotically-active nuclei. The procedure was slightly modified from a previously established protocol (Buzgariu *et al.,* 2018). *Hydra* were relaxed in 2% urethane/HM for 2 minutes, fixed with 4% paraformaldehyde/HM for 1 hour at room temperature, washed 3× in 1X PBS for 10 min, permeabilized in 0.5% Triton/PBS for 10 minutes at room temperature, blocked with 1% BSA (Sigma) in 0.1% Triton/PBS for 1 hour at room temperature. Fixed specimens were incubated with rabbit anti phospho-histone H3 antibody (1:200) (Thermo Fisher) and 1X HALT cocktail (Thermo Fisher) overnight at 4°C in blocking solution. Following incubation, specimens were washed 3× in 1X PBS for 10 min, then incubated with secondary FITC conjugated anti rabbit antibody (1:200) (Thermo Fisher), DAPI (1:5000) (Sigma) and

1X HALT cocktail in blocking solution for 2 hours at room temperature. Following incubation, specimens were washed 3× in 1X PBS for 10 min then mounted with Mowiol 4-88 (Sigma). Specimens were imaged with the Zeiss AXIO Observer D1 microscope and ZEN software. The number of fluorescent nuclei in the entire animal (excluding the tentacles) were counted manually to determine the density (fluorescent nuclei/μm^2). Sample size: N=13 and 14 for inhibitor-treated *Hydra* at 12 hpe and 24 hpe, respectively; N=14 for control *Hydra*.

Acridine orange staining

Hydra exposed to 1 μM SB 218078 (Tocris) for 12 and 24 hours were stained with acridine orange to detect apoptotic cells. Acridine orange staining was performed as previously described (Miller *et al.,* 2000). *Hydra* were incubated with 3.3 mM acridine orange (Sigma) for 15 minutes in the dark, washed 2× with HM for 10 min and mounted in Mowiol 4-88 (Sigma). Specimens were imaged with the Zeiss AXIO Observer D1 microscope and ZEN software. Fluorescence intensity (a.u.) in the entire animal (excluding the tentacles) was measured using ImageJ. Sample size: N=14 and 13 for inhibitor-treated *Hydra* at 12 hours post exposure (hpe) and 24 hpe, respectively; N=14 for control *Hydra*.

Cell macerates

Cell macerates for *Hydra* exposed to 1 μM SB 218078 (Tocris) for 12 and 24 hours were prepared as described (David, 1973). *Hydra* gastric segments (10 segments/tube) were incubated in 200 μl of maceration solution (1:1:13 ratio of glycerol, glacial acetic acid and ddH_2O) for 40 minutes at room temperature, with gentle intermittent mixing of the tube, to this 200 μl of 8% paraformaldehyde/HM were added, incubated for 20 minutes at room temperature, followed by the addition of 20 μl of 10% Tween 80 (Sigma). Aliquots of 50 μl of the final maceration solution were distributed on a poly-lysine coated glass slides and air-dried for 48 hours. Following the drying period, slides were washed 3× with 10X PBS and incubated with a 1X PBS solution containing 200 ul of 6000 nM DAPI (Sigma) and 1000 nM Mitotracker (Thermo Fisher) in the dark for 40 minutes. Following incubation, slides were washed 3× with 1X PBS and mounted in Mowiol 4-88 (Sigma). Slides were imaged using the Zeiss AXIO Observer D1 microscope and ZEN software. N=5 for each treatment group. Cells were counted manually to determine the relative proportion of each type: ectodermal epithelial cells, endodermal epithelial cells, interstitial cells, nematoblasts, nematocysts, gland cells and nerve cells (>500 cells counted for each slide).

Nematocyst staining with toluidine blue

Hydra exposed to 1 μM SB 218078 (Tocris) for 6 hours were stained with toluidine blue to detect the stenotele nematocysts. Toluidine blue staining was performed as described (Ambrosone *et al.,* 2014). *Hydra* were relaxed with 2% urethane/HM for 2 minutes, fixed with absolute ethanol for 5 minutes, washed 5× with ddH_2O for 10 minutes, then washed 2× with 10 mM Tris-Cl (pH 7.5) for 5 minutes. Next, specimens were stained with 0.01% toluidine blue (Sigma) in 10 mM Tris-Cl (pH 7.4) for 10 minutes, washed 5× with ddH_2O for 10 minutes, dehydrated in an ethanol series (for 5 minutes each at 50%, 75%, 95% in water, then twice for 100%), cleared with 1:1 ethanol: xylene for 5 minutes, and twice with 100% xylene for 10 minutes. Specimens were mounted on DPX (Sigma) and then imaged with the Zeiss AXIO Observer D1 microscope and ZEN software. Two 50 μm^2 squares were sampled in the proximal region of the tentacles; the number of stenoteles per 50 μm^2 was counted manually to determine the stenotele density. N=14 for inhibitor-treated *Hydra*; N=11 for control *Hydra*.

Peroxidase foot staining

Hydra exposed to 1 μM SB 218078 (Tocris) for 12 and 24 hours were stained for peroxidase activity to detect foot structures. Peroxidase staining was slightly modified from established protocols (Hoffmeister and Schaller, 1985). *Hydra* were fixed with 4% paraformaldehyde/HM for 20 minutes at room temperature, washed with PBT (1X PBS and 0.25% Triton X-100, pH 7.4) 2× for 10 minutes, then incubated with the foot staining solution consisting of 0.1% 3,3′-diaminobenzidine (Sigma), PBT, and 0.3% H_2O_2 for 10 minutes. The peroxidase reaction was stopped by washing with PBT 3× for 10 minutes. Specimens were imaged with the Leica M165 dissecting scope and Leica Application Imaging Suite software. Sample size: N=14 and 15 for inhibitor-treated *Hydra* at 12 hours post exposure (hpe) and 24 hpe, respectively; N=15 for control *Hydra*.

Statistical analysis

Data visualization and statistical analysis was performed using RStudio software. Shapiro and Bartlett's tests were performed to determine normality and homogeneity of variance respectively, where $P \geq 0.05$ indicated normal distribution and equal variance across samples. Two sample t-tests or Wilcoxon tests were performed to assess the difference between control and SB 218078 treated samples in the following assays: cell macerates, stenotele density, phospho H3, and acridine orange. P-values < 0.05 were considered to be statistically significant.

Acknowledgements

A.R.C would like to thank Dr. Brigitte Galliot for the introduction to the lovely Hydra *model organism. We would like to thank the Wilson lab for providing us with brine shrimp cultures and the McMaster Data Lunch group for their thoughtful discussions. This work is a result of the Undergraduate Honours Theses completed by Y.L, V.M and S.A to partially fulfill degree requirements as set by the Department of Biology at McMaster University. We would like to acknowledge our funding sources during the course of the work: Y.L by NSERC Undergraduate Student Research Award (USRA), J. Y. W and A.R.C by NSERC Discovery grant.*

References

ALVARADO AS and TSONIS PA. (2006). Bridging the regeneration gap: genetic insights from diverse animal models. *Nat Rev Gen* 7: 873.

AMBROSONE A, SCOTTO DI VETTIMO MR, MALVINDI MA, ROOPIN M, LEVY O, MARCHESANO V, POMPA PP, TORTIGLIONE C and TINO A. (2014). Impact of amorphous SiO2 nanoparticles on a living organism: morphological, behavioral, and molecular biology implications. *Front Bioeng Biotechnol* 29: 37.

ARVIZU F, AGUILERA A and SALGADO LM. (2006). Activities of the protein kinases STK, PI3K, MEK, and ERK are required for the development of the head organizer in *Hydra magnipapillata. Differentiation* 74: 305-312.

AUFSCHNAITER R, WEDLICH-SÖLDNER R, ZHANG X and HOBMAYER B. (2017). Apical and basal epitheliomuscular F-actin dynamics during Hydra bud evagination. *Biol Open* 6:1137-1148.

BARBOULE N, LAFON C, CHADEBECH P, VIDAL S and VALETTE A. (1999). Involvement of p21 in the PKC-induced regulation of the G2/M cell cycle transition. *FEBS Lett* 444: 32-37.

BARVE A, GHASKADBI S and GHASKADBI S. (2013a). Structural and sequence similarities of Hydra Xeroderma Pigmentosum A protein to human homolog suggest early evolution and conservation. *Biomed Res Int* 2013: 854745.

BARVE A, GHASKADBI S and GHASKADBI S. (2013b). Conservation of the nucleotide excision repair pathway: characterization of Hydra Xeroderma Pigmentosum group F homolog." *PLoS One* 8: e61062.

BEDELBAEVA K, SNYDER A, GOUREVITCH D, CLARK L, ZHANG XM, LEFEROVICH J, CHEVERUD JM, LIEVERMAN P and HEBER-KATZ E. (2010). Lack of p21 expression links cell cycle control and appendage regeneration in mice. *Proc Natl Acad Sci U S A* 107: 5845-5850.

BLASIUS M, FORMENT JV, THAKKAR N, WAGNER SA, CHOUDHARY C and JACKSON SP. (2011). A phospho-proteomic screen identifies substrates of the checkpoint kinase Chk1. *Genome Biol* 12: R78.

BODE HR. (1996). The interstitial cell lineage of Hydra: a stem cell system that arose early in evolution. *J Cell Sci* 109: 1155-1164.

BODE HR. (2009). Axial patterning in Hydra. *Cold Spring Harb Perspect Biol* 1: a000463.

Boehm AM, Rosenstiel P and Bosch TC. (2013). Stem cells and aging from a quasi-immortal point of view. *BioEssays* 35: 994-1003.

BOSCH TCG. (2007). Why polyps regenerate and we don't: towards a cellular and molecular framework for Hydra regeneration. *Dev Biol* 303: 421-433.

BROUN M, GEE L, REINHARDT B and BODE HR. (2005). Formation of the head organizer in Hydra involves the canonical Wnt pathway. *Development* 132: 2907-2916.

BUZGARIU W, CRESCENZI M and GALLIOT B. (2014). Robust G2 pausing of adult stem cells in Hydra. *Differentiation* 87: 83-99.

BUZGARIU W, AL HADDAD S, TOMCZYK S, WENGER Y and GALLIOT B. (2015). Multi-functionality and plasticity characterize epithelial cells in Hydra. *Tissue Barriers* 3: e1068908.

BUZGARIU W, WENGER Y, TCACIUC N, CATUNDA-LEMOS AP and GALLIOT B. (2018). Impact of cycling cells and cell cycle regulation on Hydra regeneration. *Dev Biol* 433: 240-253.

CAMACHO C, COULOURIS G, AVAGYAN V, MA N, PAPADOPOULOS J, BEALER K and MADDEN TL. (2009). BLAST+: architecture and applications. *BMC Bioinform* 10: 421.

CAMPBELL RD. (1967). Tissue dynamics of steady state growth in Hydra littoralis. II. Patterns of tissue movement. *J Morphol* 121: 19-28.

CARDENAS M, FABILA YV, YUM S, CERBON J, BÖHMER FD, WETZKER R, FUJISAWA T, BOSCH TC and SALGADO LM. (2000). Selective protein kinase inhibitors block head-specific differentiation in Hydra. *Cell Signal* 12: 649-658.

CARDENAS M and SALGADO LM. (2003). STK, the src homologue, is responsible for the initial commitment to develop head structures in Hydra. *Dev Biol* 264: 495-505.

CARRASSA L, MONTELATICI E, LAZZARI L, ZANGROSSI S, SIMONE M, BROGGINI M and DAMIA G. (2010). Role of Chk1 in the differentiation program of hematopoietic stem cells. *Cell Mol Life Sci* 67: 1713-1722.

CHAPMAN JA, KIRKNESS EF, SIMAKOV O, HAMPSON SE, MITROS T, WEINMAIER T, RATTEI T, BALASUBRAMANIAN PG, BORMAN J, BUSAM D and DISBENNETT K. (2010). The dynamic genome of Hydra. *Nat* 464: 592.

CHEN JS, LIN SY, TSO WL, YEH GC, LEE WS, TSENG H, CHEN LC and HO YS. (2006). Checkpoint kinase 1-mediated phosphorylation of Cdc25C and bad proteins are involved in antitumor effects of loratadine-induced G2/M phase cell-cycle arrest and apoptosis. *Mol Carcinog* 45: 461-478.

CHERA S, GHILA L, DOBRETZ K, WENGER Y, BAUER C, BUZGARIU W, MARTINOU JC and GALLIOT B. (2009). Apoptotic cells provide an unexpected source of Wnt3 signaling to drive Hydra head regeneration. *Dev Cell* 17: 279-289.

DAŃKO MJ, KOZŁOWSKI J and SCHAIBLE R. (2015). Unraveling the non-senescence phenomenon in Hydra. *J Theor Biol* 382: 137-49.

DAVID CN. (1973). A quantitative method for maceration of Hydra tissue. *Wilhelm Roux Arch Entwickl Mech Org* 171: 259-268.

DIPAOLA RS. (2002). To arrest or not to G2-M cell-cycle arrest. *Clin Cancer Res* 8: 3311-3314.

DÜBEL S, HOFFMEISTER SA and SCHALLER HC. (1987). Differentiation pathways of ectodermal epithelial cells in Hydra. *Differentiation* 35: 181-189.

EMING SA, MARTIN P and TOMIC-CANIC M. (2014). Wound repair and regeneration: mechanisms, signaling, and translation. *Sci Transl Med* 6: 265sr6.

GALANDE AA, PERWEEN N, SAIJO M, GHASKADBI SS and GHASKADBI S. (2018). Analysis of the conserved NER helicases (XPB and XPD) and UV-induced DNA damage in Hydra. *Biochim Biophys Acta Gen Subj* 1862: 2031-2042.

GALANDE AA, SAIJO M, GHASKADBI SS and GHASKADBI S. (2021). Xeroderma pigmentosum A homolog from Hydra partially complements DNA repair defect in human XPA-deficient cells. *J Biosci* 46: 48.

GALLIOT B. (2012). Hydra, a fruitful model system for 270 years. *Int J Dev Biol* 56: 411-423.

GALLIOT B. (2013). Injury-induced asymmetric cell death as a driving force for head regeneration in Hydra. *Dev Genes Evol* 223: 39-52.

GALLIOT B, BUZGARIU WC, SCHENKELAARS Q and WENGER Y. (2018). Non-developmental dimensions of adult regeneration in Hydra. *Int J Dev Biol* 62: 373-381.

GALLIOT B and CHERA S. (2010). The Hydra model: disclosing an apoptosis-driven generator of Wnt-based regeneration. *Trends Cell Biol* 20: 514-523.

GLAUBER KM, DANA CE, PARK SS, COLBY DA, NORO Y, FUJISAWA T, CHAMBERLIN AR and STEELE RE. (2013). A small molecule screen identifies a novel compound that induces a homeotic transformation in Hydra. *Development* 140: 4788-4796.

HARPER LJ, COSTEA DE, GAMMON L, FAZIL B, BIDDLE A and MACKENZIE IC. (2010). Normal and malignant epithelial cells with stem-like properties have an extended G2 cell cycle phase that is associated with apoptotic resistance. *BMC Cancer* 10: 166.

HAVAL GA, PEKHALE KD, PERWEEN N, GHASKADBI SM and GHASKADBI SS. (2020). Excess hydrogen peroxide inhibits head and foot regeneration in Hydra by affecting DNA repair and expression of essential genes. *J Biochem Mol Toxicol* 34: e22577.

HOBMAYER B, JENEWEIN M, EDER D, EDER MK, GLASAUER S, GUFLER S, HARTL M and SALVENMOSER W. (2012). Stemness in Hydra-a current perspective. *Int J Dev Biol* 56: 509-517.

HOFFMEISTER S and SCHALLER HC. (1985). A new biochemical marker for foot-specific cell differentiation in Hydra. *Roux Arch Dev Biol* 194: 453-461.

HUFNAGEL LA, KASS-SIMON G and LYON MK. (1985). Functional organization of battery cell complexes in tentacles of *Hydra attenuata*. *J Morphol* 184: 323-341.

JACKSON JR, GILMARTIN A, IMBURGIA C, WINKLER JD, MARSHALL LA and ROSHACK A. (2000). An indolocarbazole inhibitor of human checkpoint kinase (Chk1) abrogates cell cycle arrest caused by DNA damage. *Cancer Res* 60: 566-572.

KALOULIS K, CHERA S, HASSEL M, GAUCHAT D and GALLIOT B. (2004). Reactivation of developmental programs: the cAMP-response element-binding protein pathway is involved in Hydra head regeneration. *Proc Natl Acad Sci U S A* 101: 2363-2368.

KAWABE T. (2004). G2 checkpoint abrogators as anticancer drugs. *Mol Cancer Ther* 3: 513-519.

KLIMOVICH A, WITTLIEB J and BOSCH TC. (2019). Transgenesis in Hydra to characterize gene function and visualize cell behavior. *Nat Protoc* 14: 2069-2090.

LANGE C and CALEGARI F. (2010). Cdks and cyclins link G1 length and differentiation of embryonic, neural and hematopoietic stem cells. *Cell Cycle* 9: 1893-1900.

LIVSHITS A, SHANI-ZERBIB L, MAROUDAS-SACKS Y, BRAUN E and KEREN K. (2017). Structural inheritance of the actin cytoskeletal organization determines the body axis in regenerating Hydra. *Cell Rep* 18: 1410-1421.

LOMMEL M, TURSCH A, RUSTARAZO-CALVO L, TRAGESER B and HOLSTEIN TW. (2017). Genetic knockdown and knockout approaches in Hydra [Preprint]. *BioRxiv*: 230300.

MADEIRA F, PARK YM, LEE J, BUSO N, GUR T, MADHUSOODANAN N, BASUTKAR P, TIVEY AR, POTTER SC, FINN RD and LOPEZ R. (2019). The EMBL-EBI search and sequence analysis tools APIs in 2019. *Nucleic Acids Res* 47: W636-W641.

MARCUM BA and CAMPBELL RD. (1978). Development of Hydra lacking nerve and interstitial cells. *J Cell Sci* 29: 17-33.

MARTÍNEZ DE. (1998). Mortality patterns suggest lack of senescence in Hydra. *Exp Gerontol* 33: 217-225.

MANUEL GC, REYNOSO R, GEE L, SALGADO LM and BODE HR. (2006). PI3K and ERK 1-2 regulate early stages during head regeneration in Hydra. *Dev Growth Differ* 48: 129-138.

MEHTA AS and SINGH A. (2019). Insights into regeneration tool box: an animal model approach. *Dev Biol* 453: 111-129.

MILLER MA, TECHNAU U, SMITH KM and STEELE RE. (2000). Oocyte development in Hydra involves selection from competent precursor cells. *Dev Biol* 224: 326-3138.

PEKHALE K, HAVAL G, PERWEEN N, ANTONIALI G, TELL G, GHASKADBI S and GHASKADBI S. (2017). DNA repair enzyme APE1 from evolutionarily ancient Hydra reveals redox activity exclusively found in mammalian APE1. *DNA Repair* 59: 44-56.

QUINN B, GAGNÉ F and BLAISE C. (2012). Hydra, a model system for environmental studies. *Int J Dev Biol* 56: 613-625.

RAO N, JHAMB D, MILNER DJ, LI B, SONG F, WANG M, VOSS SR, PALAKAL M, KING MW, SARANJAMI B and NYE HL. (2009). Proteomic analysis of blastema formation in regenerating axolotl limbs. *BMC Biol* 7: 83.

REITER S, CRESCENZI M, GALLIOT B and BUZGARIU WC. (2012). Hydra, a versatile model to study the homeostatic and developmental functions of cell death. *Int J Dev Biol* 56: 593-604.

SCHENKELAARS Q, TOMCZYK S, WENGER Y, EKUNDAYO K, GIRARD V, BUZGARIU W, AUSTAD S and GALLIOT B. (2018). Hydra, a model system for deciphering the mechanisms of aging and resistance to aging. In *Conn's handbook of models for human aging* (Eds PM Conn and JL Ram). Academic Press, pp. 507-520.

SIEBERT S, FARRELL JA, CAZET JF, ABEYKOON Y, PRIMACK AS, SCHNITZLER CE and JULIANO CE. (2019). Stem cell differentiation trajectories in Hydra resolved at single-cell resolution. *Science* 365: eaav9314.

SUGIYAMA T and FUJISAWA T. (1978). Genetic analysis of developmental mechanisms in Hydra. II. Isolation and characterization of an interstitial cell-deficient strain. *J Cell Sci* 29: 35-52.

TANG J, ERIKSON RL and LIU X. (2006). Checkpoint kinase 1 (Chk1) is required for mitotic progression through negative regulation of polo-like kinase 1 (Plk1). *Proc Natl Acad Sci U S A* 103: 11964-11969.

TECHNAU U and STEELE RE. (2011). Evolutionary crossroads in developmental biology: Cnidaria. *Development* 138: 1447-1458.

TURWANKAR A and GHASKADBI S. (2019). VEGF and FGF signaling during head regeneration in Hydra. *Gene* 717: 144047.

VAN OUDENHOVE JJ, GRANDY RA, GHULE PN, DEL RIO R, LIAN JB, STEIN JL, ZAIDI SK and STEIN GS. (2016). Lineage-specific early differentiation of human embryonic stem cells requires a G2 cell cycle pause. *Stem Cells* 34: 1765-1775.

VOGG MC, BECCARI L, OLLÉ LI, RAMPON C, VRIZ S, PERRUCHOUD C, WENGER Y and GALLIOT B. (2019). An evolutionarily-conserved Wnt3/β -catenin/Sp5 feedback loop restricts head organizer activity in Hydra. *Nat Commun* 10: 1-15.

WALWORTH N, DAVEY S and BEACH D. (1993). Fission yeast Chk1 protein kinase links the rad checkpoint pathway to cdc2. *Nat* 363: 368.

WANG F, WANG F, ZOU Z, LIU D, WANG J and SU Y. (2011). Active deformation of apoptotic intestinal epithelial cells with adhesion-restricted polarity contributes to apoptotic clearance. *Lab Invest* 91: 462.

WENGER Y and GALLIOT B. (2013a). Punctuated emergences of genetic and phenotypic innovations in eumetazoan, bilaterian, euteleostome, and hominidae ancestors. *Genome Biol Evol* 5: 1949–1968.

WENGER Y and GALLIOT B. (2013b). RNAseq versus genome-predicted transcriptomes: a large population of novel transcripts identified in an Illumina-454 Hydra transcriptome. *BMC Genomics* 14: 204.

WENGER Y, BUZGARIU W and GALLIOT B. (2016). Loss of neurogenesis in Hydra leads to compensatory regulation of neurogenic and neurotransmission genes in epithelial cells. *Philos Trans R Soc B* 371: 20150040.

WENGER Y, BUZGARIU W, PERRUCHOUD C, LOICHOT G and GALLIOT B. (2019). Generic and context-dependent gene modulations during Hydra whole body regeneration [Preprint]. *BioRXiv*: 587147.

WILSKER D, PETERMANN E, HELLEDAY T and BUNZ F. (2008). Essential function of Chk1 can be uncoupled from DNA damage checkpoint and replication control. *Proc Natl Acad Sci U S A* 105: 20752-20757.

ZAUGG K, SU YW, REILLY PT, MOOLANI Y, CHEUNG CC, HAKEM R, HIRAO A, LIU Q, ELLEDGE SJ and MAK TW. (2007). Cross-talk between Chk1 and Chk2 in double-mutant thymocytes. *Proc Natl Acad Sci U S A* 104: 3805-3810.

ZHANG Y and HUNTER T. (2014). Roles of Chk1 in cell biology and cancer therapy. *Int J Cancer* 134: 1013–1023.

ZHAO B, BOWER MJ, MCDEVITT PJ, ZHAO H, DAVIS ST, JOHANSON KO, GREEN SM, CONCHA NO and ZHOU BB. (2002). Structural basis for Chk1 inhibition by UCN-01. *J Biol Chem* 277: 46609-46615.

Further Related Reading, published previously in the *Int. J. Dev. Biol.*

Cell signaling molecules in hydra: insights into evolutionarily ancient functions of signaling pathways
Surendra Ghaskadbi
Int. J. Dev. Biol. (2020) 64: 141-149
https://doi.org/10.1387/ijdb.190243sg

Hydra, a model system for environmental studies
Brian Quinn, François Gagné, Christian Blaise
Int. J. Dev. Biol. (2012) 56: 613-625
https://doi.org/10.1387/ijdb.113469bq

Hydra, a fruitful model system for 270 years
Brigitte Galliot
Int. J. Dev. Biol. (2012) 56: 411-423
https://doi.org/10.1387/ijdb.120086bg

Non-developmental dimensions of adult regeneration in *Hydra*
Brigitte Galliot, Wanda Buzgariu, Quentin Schenkelaars and Yvan Wenger
Int. J. Dev. Biol. (2018) 62: 373-381
https://doi.org/10.1387/ijdb.180111bg

***Hydra*, a versatile model to study the homeostatic and developmental functions of cell death**
Silke Reiter, Marco Crescenzi, Brigitte Galliot and Wanda Buzgariu
Int. J. Dev. Biol. (2012) 56: 593-604
https://doi.org/10.1387/ijdb.123499sr

Components, structure, biogenesis and function of the Hydra extracellular matrix in regeneration, pattern formation and cell differentiation
Michael P. Sarras (Jr)
Int. J. Dev. Biol. (2012) 56: 567-576
https://doi.org/10.1387/ijdb.113445ms

Stemness in Hydra - a current perspective
Bert Hobmayer, Marcell Jenewein, Dominik Eder, Marie-Kristin Eder, Stella Glasauer, Sabine Gufler, Markus Hartl and Willi Salvenmoser
Int. J. Dev. Biol. (2012) 56: 509-517
https://doi.org/10.1387/ijdb.113426bh